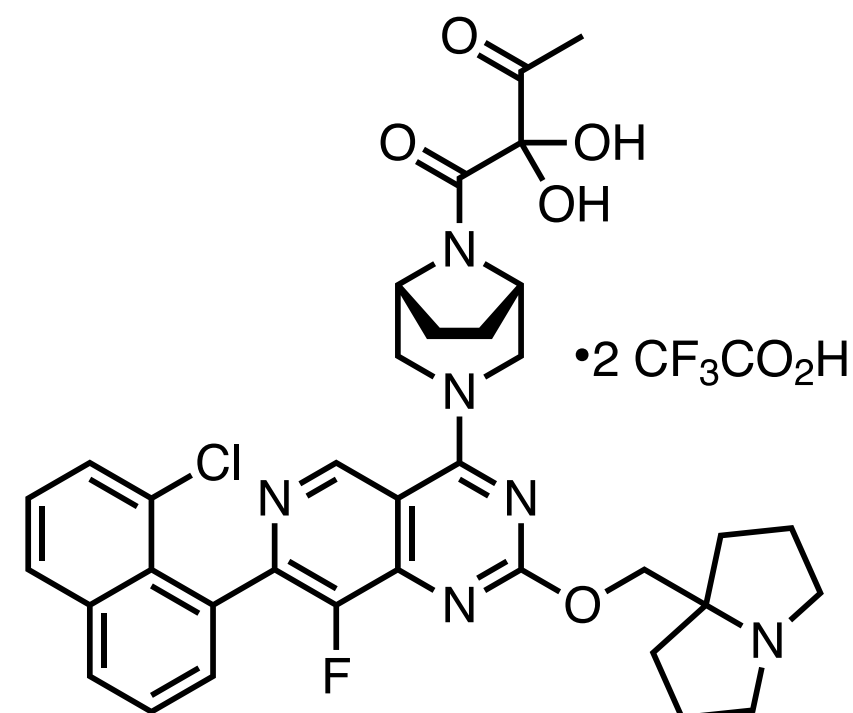


# Small Molecules of the Month

August 2022

drug  
hunter



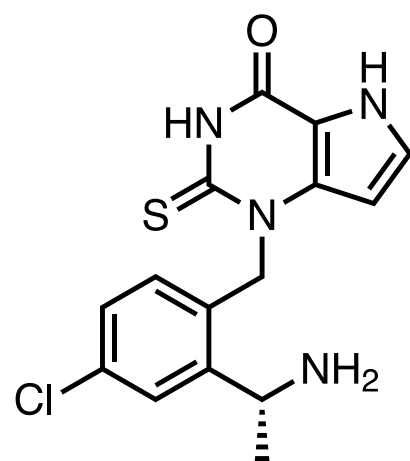
01	Compound 3	KRAS <sup>G12R</sup>	UCSF
02	AZD4831	MPO	AstraZeneca
03	obicetrapib	CETP	Monash University
04	SPH3127	Renin	Mitsubishi Tanabe & Shanghai Pharmaceuticals
05	compound 19	DHODH	Janssen
06	GNE-064	SMARCA2/4 & PBRM1	Genentech & Constellation
07	ACT-660602	CXCR3	Idorsia Pharmaceuticals
08	compound 23	Cat K	Merck & Co
09	compound 7	20S Proteasome	Novartis
10	compound 6	YAP-TEAD	Novartis





# AZD4831

MPO



**Context.** [AZD4831](#) (AstraZeneca) is an oral covalent myeloperoxidase (MPO) inhibitor being developed for heart failure. Almost half of chronic heart disease patients suffer from heart failure with a preserved ejection fraction (HFpEF) and have an estimated [five-year mortality rate of 75%](#). Improvement in vascular structure could help these patients, and targeting MPO is a potential way to achieve this. [Extracellular MPO](#) causes tissue damage by catalyzing the formation of reactive oxygen species. One of the first tool molecules, [4-aminobenzoic acid hydrazide](#), expanded our understanding of MPO's mechanism of action and propelled the development of more potent inhibitors such as the thiopyrimidinone [PF-06282999](#). The structure of AZD4831 was [first disclosed](#) at the fall ACS meeting in Chicago this year.

**Target.** [Myeloperoxidase](#) is an antimicrobial heme peroxidase, and a [key component of the innate immune response](#) expressed predominantly by neutrophils in lysosomes and secreted into the extracellular milieu. MPO is [localized to atherosclerotic lesions](#), and elevated MPO levels are associated with oxidative stress, and inflammation, and are an [independent predictor of heart attack](#). Unsurprisingly, MPO has been [implicated](#) in various chronic inflammatory conditions; however drugging it is challenged by the presence of [closely-related peroxidases](#) thyroid peroxidase, eosinophil peroxidase, and lactoperoxidase. AstraZeneca scientists sought an oral compound with strong MPO-selectivity and limited brain-penetrating properties, presumably to minimize nonspecific covalent binding in the brain.

**Mechanism of Action.** During the halogenation cycle, native MPO is [activated by hydrogen peroxide](#), which converts the enzyme to the highly reactive species, "compound I." "Compound I," in turn, reacts with various halogen ions to form the corresponding hypohalous acid. The generated hypohalous acid then reduces MPO back to its native state. Alternatively, "compound I" can act as a peroxidase, leading to the generation of a redox intermediate, "compound II," which is in turn reduced to its native stage; this process is the peroxidase cycle. Reversible inhibitors have been shown to [compete with the halogenation cycle](#) but cannot prevent the conversion of "compound II" back to the MPO native state by endogenous substrates. AstraZeneca scientists sought mechanism-based compounds, termed "suicide substrates," that [irreversibly bind with "compound II"](#), irreversibly inactivating the enzyme.

**Hit-Finding Strategy.** The irreversible MPO inhibitors [verdiperstat](#), [PF-06282999](#), [AZD5904](#) were used as inspiration for starting points. Verdiperstat is currently in a [Ph. III](#) trial for multiple system atrophy, a PF-06282999 Ph. I trial was terminated due to concerns over the [induction of CYP3A4](#), and AZD5904 has completed a [Ph. I trial](#). With the aim of an oral, low-dose, once-daily, and highly selective MPO inhibitor (over TPO) with limited brain penetration, the scientists at AstraZeneca started by replacing the aliphatic side chains of verdiperstat and AZD5904 with a benzylic moiety ("compound 4"). Activity was determined using purified MPO and TPO in an in vitro chemiluminescent assay.

oral MPO covalent inhibitor

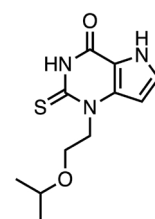
Ph. I/II candidate in HFpEF

previous literature and selectivity opt

*J. Med. Chem.*

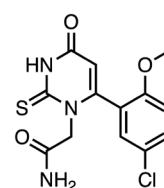
AstraZeneca, Gothenburg, SE

featured article: <https://doi.org/10.1021/acs.jmedchem.1c02141>



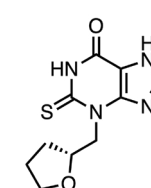
**Verdiperstat**

MPO IC<sub>50</sub> = 630 nM  
TPO IC<sub>50</sub> = 0.99 μM



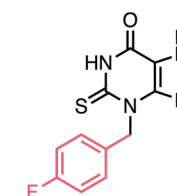
**PF-06282999**

MPO IC<sub>50</sub> = 187 nM  
TPO IC<sub>50</sub> = 0.99 μM



**AZD5904**

MPO IC<sub>50</sub> = 279 nM  
TPO IC<sub>50</sub> = 2.4 μM

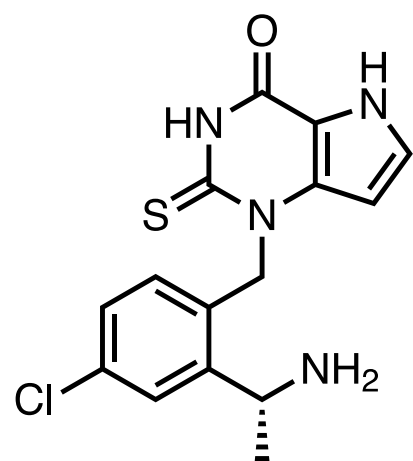


**Compound 4**

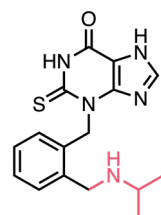
MPO IC<sub>50</sub> = 32.0 nM  
TPO IC<sub>50</sub> = 0.59 μM

# AZD4831

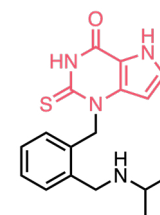
MPO



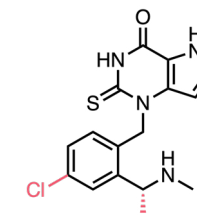
**Lead Optimization.** Initial optimization by exploration of phenyl substituents indicated a preference for a strongly basic secondary amine at the *ortho* position, with as much as 10-fold greater selectivity for MPO than TPO (“compound 5”). This selectivity was further improved by the replacement of the thioxanthine scaffold with a deaza thioxanthine (“compound 6”). Chlorination at the 4-position of the phenyl ring and addition of a methyl group at the benzylic position next to the amine improved potency but at the cost of selectivity (“compound 15”). However, when the amine was demethylated, both potency and selectivity returned (AZD4831).



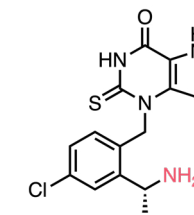
**Compound 5**  
MPO IC<sub>50</sub>: 38.6 nM  
TPO IC<sub>50</sub>: 4.2 μM



**Compound 6**  
MPO IC<sub>50</sub>: 30.9 nM  
TPO IC<sub>50</sub>: 8.1 μM



**Compound 15**  
MPO IC<sub>50</sub>: 12.7 nM  
TPO IC<sub>50</sub>: 1.1 μM



**AZD4831**  
MPO IC<sub>50</sub>: 1.5 nM  
TPO IC<sub>50</sub>: 0.69 μM

**Binding Mode.** The structure of AZD4831 bound to native MPO was not disclosed; however, the bound structures of related compounds, AZD5904 (**PDB:7NI1**) and “compound 9” (**PDB:7NI3**), were. **As expected**, these crystal structures show the thioxanthine moiety interacting through hydrogen bonds with the heme carboxylate group near the Arg239 residue. No other significant interactions with the protein were seen.

**Preclinical Pharmacology.** AZD4831 dose-dependently inhibits MPO activity in lavage fluid, as measured by chemiluminescent assay following AZD4831 pretreatment in a mouse model of **zymosan-induced neutrophilic peritonitis**. Long-term toxicological studies in rats (up to 6 months) and dogs (up to 9 months) in doses up to 125 mg/kg did not reveal any notable adverse events.

**Clinical Development.** AZD4831 has been **evaluated** in several completed and ongoing Ph. I studies (**NCT05236543**, **NCT05052710**, **NCT04232345**, **NCT04949438**, and **NCT0440709**), while a **Ph. IIb/III** study is also currently underway. In the Ph. II randomized, double-blind, placebo-controlled, parallel-group **SATELLITE study** which evaluated the drug in 41 patients with heart failure, a **69% (95% CI: 36.3, 85.0) reduction** in MPO activity in the AZD4831 group from baseline to day 30 was observed. The trial was **terminated** early based on data showing target engagement and an acceptable safety profile. In the follow-up randomized, double-blind, placebo-controlled Ph. IIb/III **ENDEAVOR trial**, AZD4831 is being evaluated in heart failure patients with a left ventricular ejection fraction of at least 40%. The study is expected to enroll ~660 patients in the first part, Part A, who will receive 2.5 or 5 mg of the drug or placebo, while ~825 patients are planned to be enrolled in Part B who will be dosed based on the findings in Part A. Key primary endpoints include the Kansas City Cardiomyopathy Questionnaire – Total Symptom Score at 16 and 24 weeks, and the six-minute walk distance at 16 and 24 weeks.

**Patent.** Thioxanthine-based inhibitors of MPO as AZD4831 were described by the AstraZeneca patent **WO2016087338A1**. The US patent **US9616063B2** was granted in April 2017 and is valid until November 2035.

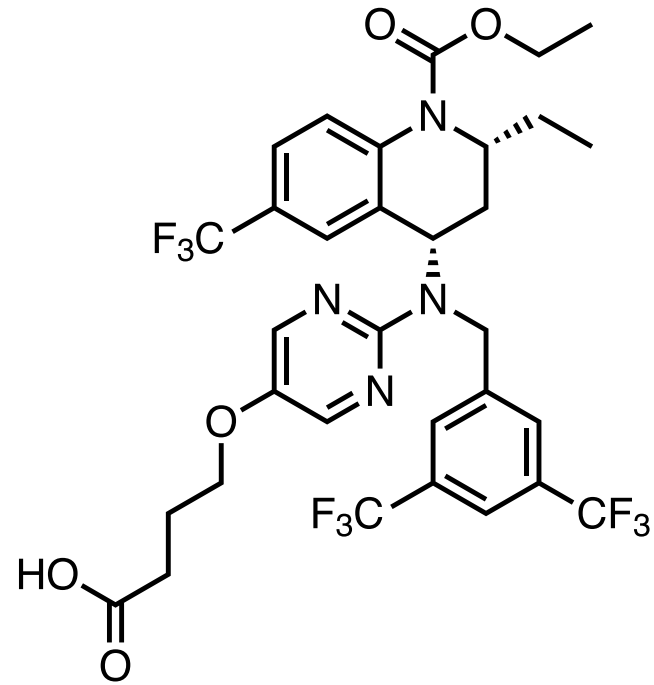
oral MPO covalent inhibitor  
Ph. IIb/III candidate in HFpEF  
previous literature and selectivity opt  
*J. Med. Chem.*

AstraZeneca, Gothenburg, SE

featured article: <https://doi.org/10.1021/acs.jmedchem.1c02141>

# Obicetrapib

## CETP



oral CETP inhibitor

Ph. III candidate in cardiology

Signif. lipid lowering effect at 5 mg PO QD

*Nat. Med.*

Monash University, Clayton, AU

NewAmsterdam Pharma B.V., Naarden, NL

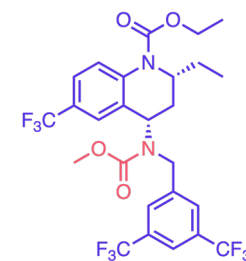
featured article: <https://doi.org/10.1038/s41591-022-01936-7>

**Context.** **Obicetrapib** (Monash University and NewAmsterdam Pharma) is an oral selective cholesteryl ester transfer protein (CETP) inhibitor being developed for dyslipidemia. Patients with high cardiovascular risk typically aim to lower cholesterol with a combination of statins, diet, and exercise, **but this is often not enough**. A **foundational study in 1990** observed that individuals with CETP mutations showed lower LDL cholesterol and increased levels of HDL cholesterol, leading to the **development of CETP inhibitors** such as torcetrapib, dalcetrapib, evacetrapib, and anacetrapib. Off-target effects or lack of efficacy stalled the development of torcetrapib, dalcetrapib, and evacetrapib while anacetrapib reduced coronary events but was associated with **adipose tissue retention** making anacetrapib inappropriate for frequent dosing. The next generation CETP inhibitor, obicetrapib, demonstrated **greater efficacy and bioavailability** with a terminal half-life suitable for daily administration. A recent **Mendelian randomization study** noted that failure of past CETP inhibitors is compound rather than target-related, and CETP inhibition is expected to reduce the risk of several CV endpoints but potentially increase age-related macular degeneration risk.

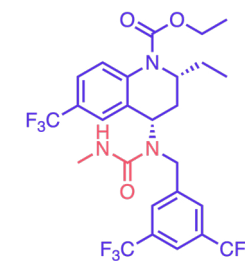
**Target.** **CETP** is a glycoprotein present in plasma that mediates the bidirectional transfers of cholesteryl esters and triglycerides between plasma lipoproteins (HDLs, VLDLs, and LDLs). Deficiency of the protein has been **associated with** significantly higher levels of HDL cholesterol and reduced levels of LDL cholesterol which reduces the risk of atherosclerosis. Consequently, CETP is a **widely-studied** studied cardiovascular disease target, although an inhibitor for the protein has yet to be approved.

**Mechanism of Action.** Inhibition of CETP **reduces the lipid transfer processes** mediated by the protein, subsequently increasing the concentration of HDL cholesterol and decreasing the concentration of VLDL and LDL cholesterol. Although **previous inhibitors** have **increased HDL and decreased LDL levels in patients**, their success has been challenged by **off-target toxicities** such as plasma aldosterone modulation in the case of torcetrapib or unimproved/worsened clinical outcomes. A recent **study** suggested that the failures of CETP inhibitors may not be due to the target but rather with the compounds themselves, which may suffer from either a lack of target engagement or competing off-target liabilities.

**Hit-Finding Strategy.** Inspiration for obicetrapib, previously named AMG-899 and TA-8995, came from **torcetrapib**. Torcetrapib ultimately reached Ph. III clinical trials as a combination with atorvastatin; however, it was prematurely terminated due to an increase in the risk of mortality and morbidity in the **torcetrapib/atorvastatin group over the atorvastatin group alone**. The full story on the design and development of obicetrapib has not been fully disclosed; however, there is an **account of its creation** (in Japanese) from scientists at Mitsubishi Tanabe. They hoped to optimize a few of torcetrapib's physical properties, such as low solubility and the need for special formulation technology to ensure proper oral bioavailability. In their attempt to design a compound that maintained CETP inhibitory activity with improved physical properties, they searched for sites that would allow for hydrophilic substituents, ultimately finding that substitution of the carbamate into a urea ("compound 2") was well tolerated.

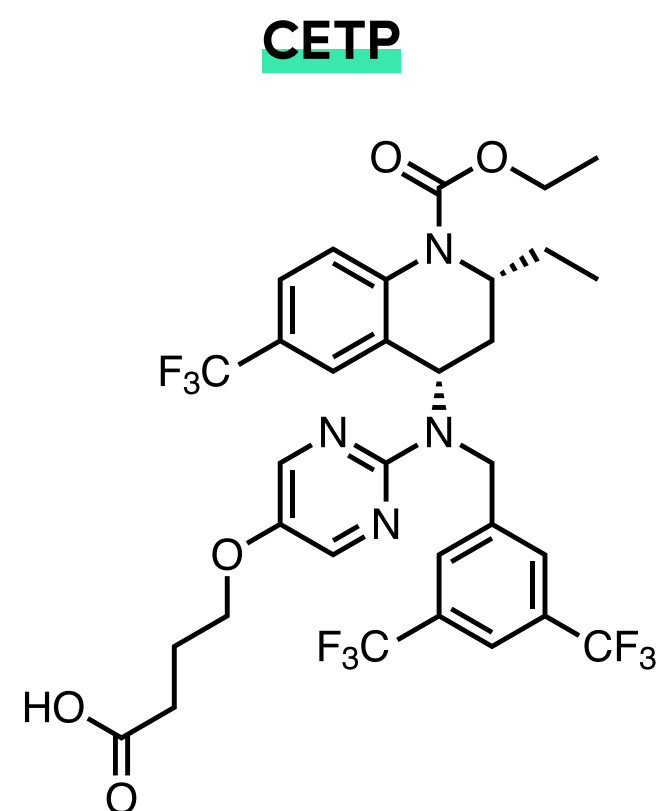


**Torcetrapib**  
CETP IC<sub>50</sub> = 55 nM

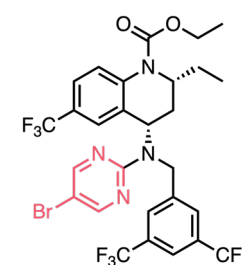


**Compound 2**  
CETP IC<sub>50</sub> = 270 nM

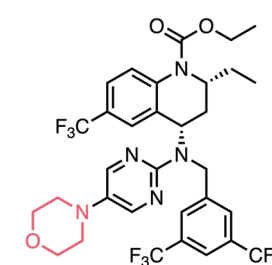
# Obicetrapib



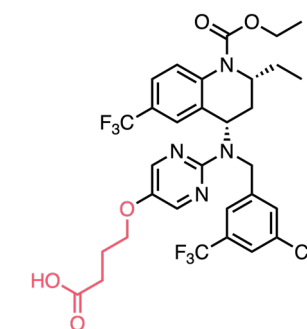
**Lead Optimization.** Initial optimization of “compound 2” began with the substitution of the urea with a bioisosteric pyrimidine (“compound 3”). Not only did this improve potency, but it also demonstrated that larger substituents were well-tolerated. Solubility was enhanced by the addition of a morpholine substituent at the expense of a minor drop in potency (“compound 4”). However, conversion of the morpholine into a carboxylic acid greatly improved potency, leading to obicetrapib.



**Compound 3**  
CETP IC<sub>50</sub> = 33 nM



**Compound 4**  
CETP IC<sub>50</sub> = 59 nM



**Obicetrapib**  
CETP IC<sub>50</sub> = 3.5 nM

**Binding Mode.** Although there is currently no co-crystal structure of CETP with obicetrapib, the structurally similar torcetrapib and “compound 2” have been disclosed (PDB: [4EWS](#), [4F2A](#)). These inhibitors occupy the [hydrophobic lipid binding tunnel](#) of CETP through predominantly hydrophobic interactions, and it's thought that obicetrapib, containing more hydrophilic groups, [bind the three polar residues](#) of the binding site, Gln199, Ser-230, and His-232. Differences in obicetrapib's binding mode and physicochemical properties (LogP 4.9 vs. anacetrapib 9.2 and evacetrapib 7.9) would confer greater solubility, affinity, and specificity and partly explain the observed potency compared to past generation inhibitors.

**Preclinical Pharmacology.** Preclinical data has not been disclosed.

**Clinical Development.** Obicetrapib is currently being [evaluated](#) in several Ph. II and III studies. In the placebo-controlled, double-blind Ph. II dose-finding [ROSE study](#), 120 patients with dyslipidemia who were on high-intensity statin therapy were randomized 1:1:1 to receive 5 mg or 10 mg of the drug or placebo for 8 weeks; patients were stratified by LDL cholesterol level. The primary endpoint was the % change in LDL cholesterol levels after 8 weeks, while key secondary endpoints were the % changes in ApoB, non-HDL cholesterol, and HDL cholesterol levels. Most patients were taking atorvastatin 40 mg (54.2%). Following the 8-week treatment period, treatment with 5 or 10 mg of obicetrapib was associated with up to 51% decrease in baseline LDL cholesterol levels vs. placebo ( $P < 0.0001$ ). Further, ApoB and non-HDL cholesterol levels were decreased by up to 30% and 44%, respectively, from baseline following treatment with obicetrapib vs. placebo ( $P < 0.0001$ ), while HDL cholesterol levels were significantly increased by up to 165% following treatment.

**Patent.** Obicetrapib and other tetrahydroquinoline CETP inhibitors were disclosed in patent [WO2015119495A](#) (Tanabe Sayaku Co.). The US patent [US7872126B2](#) is valid until September 2027. The use of obicetrapib for the treatment or prevention of cardiovascular diseases was described in patent [WO2015119495A1](#).

oral CETP inhibitor

Ph. III candidate in cardiology

Signif. lipid lowering effect at 5 mg PO QD

*Nat. Med.*

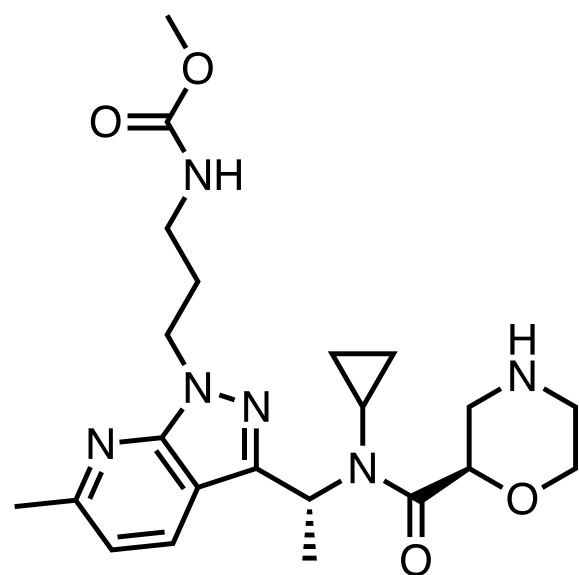
Monash University, Clayton, AU

NewAmsterdam Pharma B.V., Naarden, NL

featured article: <https://doi.org/10.1038/s41591-022-01936-7>

# SPH3127

## Renin



oral Renin Inhibitor

Ph. III candidate in essential hypertension

SBDD and PK profile opt

*J. Med. Chem.*

Mitsubishi Tanabe, Yokohama, JP

Shanghai Pharmaceuticals, Shanghai, CN

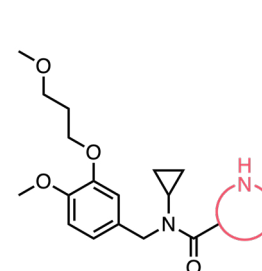
featured article: <https://doi.org/10.1021/acs.jmedchem.2c00834>

**Context.** [SPH3127](#) (Mitsubishi Tanabe and Shanghai Pharmaceuticals) is an oral direct renin inhibitor (DRI) being developed for hypertension. The [renin-angiotensin-aldosterone system](#) is responsible for regulating blood pressure. [Existing drugs treat hypertension](#) by targeting angiotensin-converting enzyme (ACE) and the angiotensin II receptor. However, these drugs can lead to a [feedback effect](#) whereby plasma serum levels become elevated. Renin, the pathway's first and rate-limiting enzyme, has been an [attractive therapeutic target for decades](#) since the [identification of peptide-like renin inhibitors and renin's structural determination](#). First and second-generation renin inhibitors were peptide analogues and transition state peptidomimetics, while third-generation compounds, guided by structure-based design, yielded non-peptidomimetic synthetic compounds such as aliskiren, which was approved in 2007. Aliskiren suffered from [low oral bioavailability](#), and other DRIs had similar high lipophilicity with MWs >500 kDa due to the [large, induced-fit binding site](#). So this team at Mitsubishi Tanabe and Shanghai Pharmaceuticals set out to develop a selective, low molecular weight small molecule renin inhibitor.

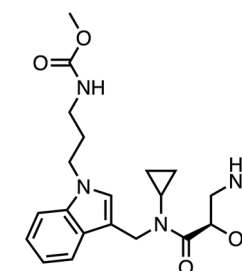
**Target.** As a central regulator of blood pressure and renal function, the [renin-angiotensin-aldosterone system \(RAAS\)](#) has been a highly-researched pathway for the discovery of anti-hypertensive agents. Unsurprisingly, several drugs [targeting proteins in the pathway](#), such as angiotensin-converting enzyme (ACE) and angiotensin receptor, have been approved for hypertension and other cardiovascular disorders. Renin is the first and rate-limiting enzyme in the pathway, and hence targeting the protein has been considered an ideal therapeutic strategy. Overexpression of renin and its downstream products has been [associated with](#) hypertension and organ damage. Renin's [active site](#) is made up of [8 pockets](#) (S1-S4 and S1'-S4') to accommodate the 8-residues N-terminus of angiotensinogen, and structural studies of [aliskiren](#) and the peptide inhibitor [CGP 38'560](#) demonstrated the importance of an additional sub-pocket S3<sup>SP</sup> for strong and selective renin inhibition.

**Mechanism of Action.** [Inhibitors of the RAAS](#) preclude the synthesis of angiotensin II, which results in the inhibition of downstream effects such as vasoconstriction and stimulation of aldosterone synthesis and release, ultimately helping to reduce blood pressure. RAAS inhibitors that target ACE and the angiotensin receptor also [increase](#) plasma renin concentration through a feedback mechanism, diminishing their overall RAAS blockade effect. The reporting scientists hypothesized that inhibiting renin with direct renin inhibitors, particularly non-peptidomimetic agents with MW <500 kDa, would produce a more pronounced anti-hypertensive effect vs. existing agents.

**Hit-Finding Strategy.** A prior [disclosure](#) from the scientists at Mitsubishi Tanabe and Shanghai Pharmaceuticals highlighted the discovery of "compound 4". Initial X-ray analysis of known DRIs bound to renin led to a core structure containing a cyclic secondary amine attached to *N*-cyclopropyl-*N*[4-methoxy-3-(3-methoxypropoxy)benzyl]amide. Optimization of this core structure ultimately led to "compound 4"; however, "compound 4" exhibited metabolic instability and time-dependent inhibition (TDI) of CYP3A4, and so became the starting point for their [current](#) drug discovery efforts.



Core Structure



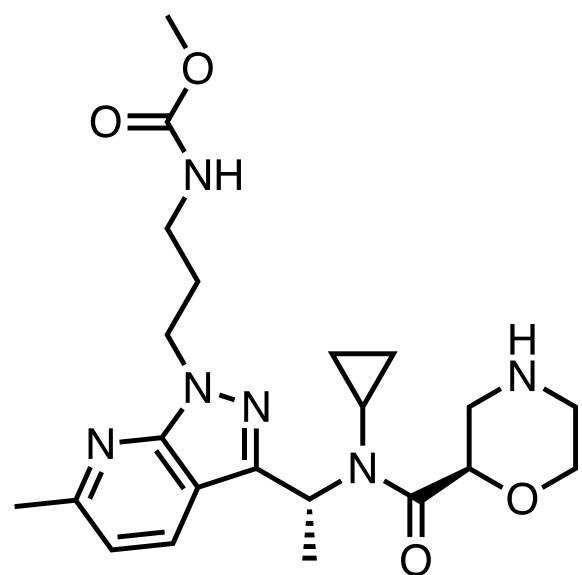
Compound 4

rh-renin IC<sub>50</sub> = 0.9 nM

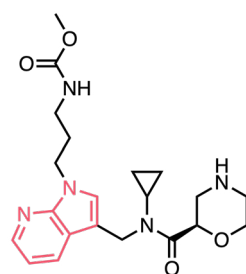
hPRA IC<sub>50</sub> = 1.8 μM

# SPH3127

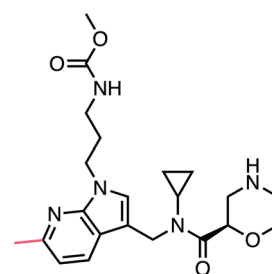
## Renin



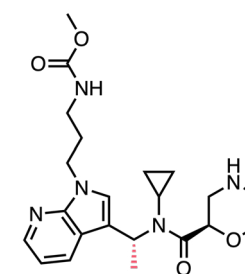
**Lead Optimization.** Optimization focused on solving the PK issues of “compound 4”, thought to be due to the indole moiety. Initial replacement of the indole with an azaindole led to a drop in renin inhibitory potency (“compound 11”), no matter where the second nitrogen was added. However, “compound 11” showed improved metabolic stability and CYP3A4 TDI, so additional optimization methods were investigated. In their [prior study](#), the introduction of a methyl substituent at the proper position slightly increased potency. The same effect held true in this study, with “compound 12” showing a roughly 7-fold improvement in potency. Still, higher potency was obtained when the methyl group was moved to the methylene at the 3-position of the azaindole (“compound 14”). Although metabolic stability and CYP3A4 TDI were improved, the bioavailability of “compound 14” was somewhat modest (F = 10%, in rats). The researchers hypothesized that correctly balancing the basicity and lipophilicity might improve oral bioavailability without diminishing metabolic stability. To this end, the optimizations of “compounds 12 and 14” were combined, and a third nitrogen was added to the azaindole, leading to SPH3127 (F = 24%, in rats).



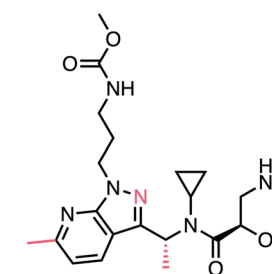
**Compound 11**  
rh-renin IC<sub>50</sub> = 3.1 nM  
hPRA IC<sub>50</sub> = 19 μM



**Compound 12**  
rh-renin IC<sub>50</sub> = 0.8 nM  
hPRA IC<sub>50</sub> = 2.6 μM



**Compound 14**  
rh-renin IC<sub>50</sub> = 0.4 nM  
hPRA IC<sub>50</sub> = 0.7 μM



**SPH3127**  
rh-renin IC<sub>50</sub> = 0.4 nM  
hPRA IC<sub>50</sub> = 0.45 μM

**Binding Mode.** X-ray cocrystal structure of SPH3127 bound to renin (**PDB:7XGP**) displayed relevant hydrophobic interactions and hydrogen bonds in the catalytic site of renin. The amine of the morpholine ring interacts with Asp32 and Asp215 residues, whereas the oxygen, with Ser76 residue. Additional hydrogen bonds can be observed between the SPH3127 carbamate NH functional group and renin Gly-217 carbonyl oxygen of the S3sp subpocket.

**Preclinical Pharmacology.** SPH3127 potently inhibited plasma renin activity (IC<sub>50</sub> = 0.46 nM) and had a bioavailability of 16% in cynomolgus monkeys pretreated with a low-sodium diet and furosemide to induce hypertension. SPH3127 also significantly reduced systolic blood pressure by at least 20 mmHg up to 6 h post-administration of 1 and 3 mg/kg. At a dose of 3 mg/kg, a significant hypotensive effect was maintained up to 16 h post-dose, with a 10 mg/kg dose maintaining the drug's hypotensive effects up to 24 h post-dose.

**Clinical Development.** Completed [Ph. I studies](#) have demonstrated the sustained plasma renin suppressive potential of the drug as well as its tolerability in patients with hypertension. A [Ph. II study](#) evaluating SPH3127 in 120 patients with mild-moderate essential hypertension has also been completed. Patients in the study were randomized 1:1:1:1 to either a low, mid, or high dose of the drug or placebo, with the primary endpoints being the changes in seated systolic blood pressure and seated diastolic blood pressure following 8 weeks of treatment. Although data from this study are yet to be disclosed, a currently ongoing follow-up [Ph. III study](#) suggests that the Ph. II trial may have had positive results.

**Patent.** SPH3127 and other morpholine derivatives were disclosed in the Shanghai Pharmaceuticals Holding Co Ltd patent [WO2014042263A1](#). The US patent [US9556159B2](#) is valid until September 2033.

oral Renin Inhibitor

Ph. III candidate in essential hypertension

SBDD and PK profile opt

*J. Med. Chem.*

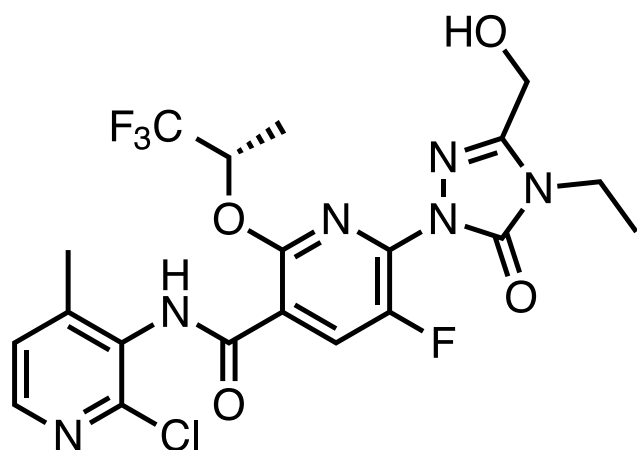
Mitsubishi Tanabe, Yokohama, JP

Shanghai Pharmaceuticals, Shanghai, CN

featured article: <https://doi.org/10.1021/acs.jmedchem.2c00834>

# Compound 19

## DHODH



**Context.** “[Compound 19](#)” (Janssen) is an oral dihydroorotate dehydrogenase (DHODH) inhibitor being developed for acute myelogenous leukemia (AML). DHODH is a ubiquitously expressed, essential enzyme in the de novo pyrimidine biosynthesis pathway. Despite its ubiquitous expression and lack of known mutations or overexpression in cancer, [DHODH](#) has been [explored](#) as a potential target, primarily because malignant cells seem to be more reliant on de novo pyrimidine biosynthesis. Although DHODH inhibitors have been explored in solid tumors, their use in liquid tumors, such as AML, is much more promising. [Fewer than 30% of patients](#) survive for more than 5 years with AML. One hallmark of AML is cell differentiation arrest, and treatment of AML patients with acute promyelocytic leukemia (APL) with [all-trans retinoic acid to induce chromosomal translocation](#) was shown to lift this differentiation blockade, but the effect was limited to APL-specific disease. [Inhibitors](#) of DHODH such as [brequinar](#) have been shown to induce differentiation, indicating that this may be a therapeutic approach for treating AML and has propelled the development of newer generation drugs like [BAY 2402234](#), [ASLAN003](#), [emvododstat](#), and Janssen’s “compound 19”. [Recent FDA approval of treatments](#) targeting mutation-driven AML is encouraging for AML treatment but highlights the need for more general treatments. “Compound 19” is one of the latest additions to the growing list of discoveries from hits initially identified by virtual screening.

**Target.** [DHODH](#) is a ubiquitously-expressed iron-containing flavin-dependent enzyme that plays a pivotal role in the de novo synthesis of pyrimidines. As key generator of [pyrimidine nucleotides](#) which are essential for tumor progression, DHODH is considered an ideal oncotarget. The role of the DHODH in AML was serendipitously [unraveled](#) in a high-throughput phenotypic screen where inhibitors targeting the protein reduced leukemic cell burden, decreased levels of leukemia-initiating cells, and improved survival. One of the compounds from the screen, [brequinar](#), is currently the most advanced DHODH inhibitor.

**Mechanism of Action.** Treatment with the DHODH inhibitor brequinar [led to](#) the depletion of pyrimidines and downstream metabolites, ultimately promoting AML tumor cell death. Molecularly, the drug caused increased differentiation of tumor cells which decreased the levels of leukemia-initiation cells; however, the mechanism linking the inhibition of pyrimidine synthesis with myeloid differentiation is still being [actively investigated](#).

**Hit-Finding Strategy.** The Janssen team used [Ligandscout 3D](#), a virtual screening tool that leverages the PDB to predict pharmacophores based on a defined set of chemical features and volume constraints, to screen their library of ~700,000 compounds. Crystal structures of two small molecules, (R)-HZ05 ([PDB:6ET4](#)) and desfluoro brequinar ([PDB:1D3G](#)), were used as inputs for Ligandscout 3D. 132 compounds came out of the screen, and were tested at 20  $\mu\text{M}$  in a biochemical DHODH colorimetric assay; 12 of these compounds displayed >50% inhibition. “Compound 5” showed the most promise, with a biochemical  $\text{IC}_{50} = 1.4 \mu\text{M}$  and [lipophilic ligand efficiency](#) (LLE) of 3.2, however, it suffered from low solubility (<4  $\mu\text{M}$  at pH 7).

oral DHODH inhibitor

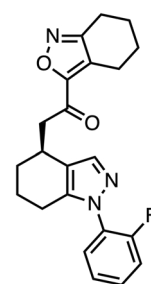
tumor growth inhibition in xenograft models

from virtual screening and SBDD

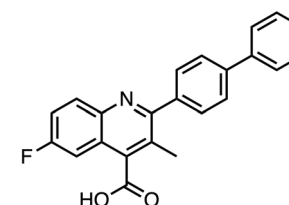
*J. Med. Chem.*

Janssen, Spring House, PA

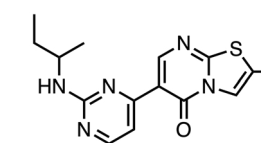
featured article: <https://doi.org/10.1021/acs.jmedchem.2c00788>



(R)-HZ05



Desfluoro Brequinar

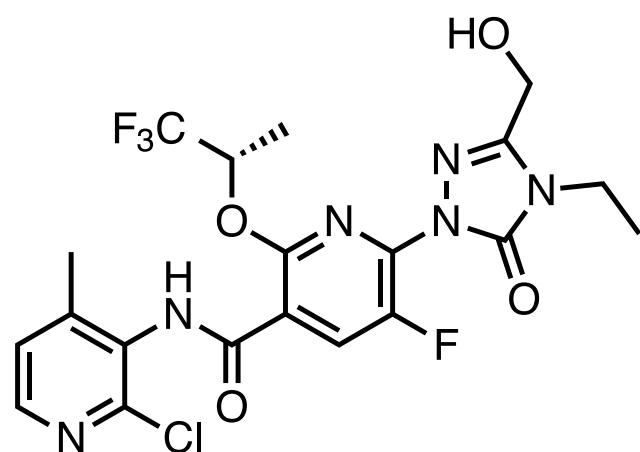


Compound 5

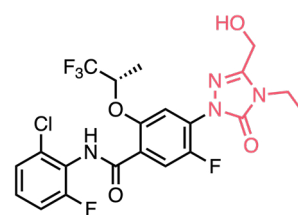
DHODH  $\text{IC}_{50} = 14.00 \text{ nM}$   
LLE = 3.2

# Compound 19

## DHODH

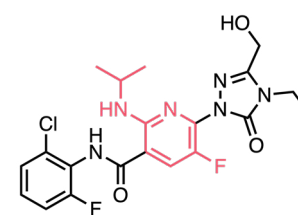


**Lead Optimization.** The docking pose of “compound 5” with DHODH suggested the thiazolopyrimidinone was in proximity to Glu47 and Tyr356, similar to a [recently published](#) DHODH inhibitor “compound 3”. Combining the structural features of these two compounds led to “compound 6”, which had comparable activity to “compound 5”, but demonstrated an improved LLE. Optimization of “compound 6” began by testing a variety of sidechains as an isopropylamine replacement. “Compound 8”, with a simple isopropyl ether, significantly boosted potency in both biochemical and cellular assays (MOLM-13 cells). A number of cyclic ethers were tried, but all showed a significant loss of potency. However, when the isopropoxy group was substituted with a trifluoromethyl isopropyl ether, nanomolar biochemical and cellular potency returned (“compound 11”). Although “compounds 8 and 11” had high potency, their solubility was still not optimal (<4  $\mu\text{M}$  at pH 7). Revisiting the structural analysis of “compound 6”, the chlorofluoroaniline moiety was predicted to occupy an “exit” vector, indicating it might be amenable to solubilizing modifications. Ultimately, substitution of the *ortho*-fluorine with a methyl group and conversion of the benzene to a pyridine led to “compound 19,” which was highly soluble, stable in human liver microsomes ( $Cl_{int} < 1.9$ ), and potent in both biochemical and cellular assays.



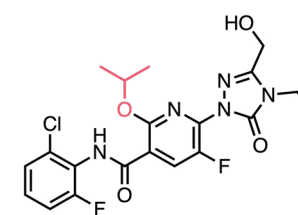
**Compound 3**

DHODH  $IC_{50}$  = 1.2 nM  
LLE = 7.1



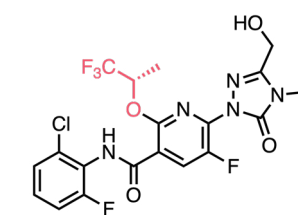
**Compound 6**

DHODH  $IC_{50}$  = 3600 nM  
MOLM-13  $IC_{50}$  = 200 nM  
LLE = 4.1



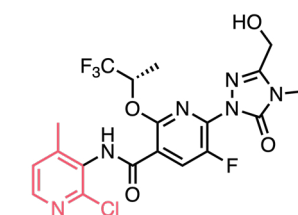
**Compound 8**

DHODH  $IC_{50}$  = 0.5 nM  
MOLM-13  $IC_{50}$  = 0.2 nM  
LLE = 8.18



**Compound 11**

DHODH  $IC_{50}$  = 0.2 nM  
MOLM-13  $IC_{50}$  = 0.16 nM  
LLE = 8.06



**Compound 19**

DHODH  $IC_{50}$  = 1.1 nM  
MOLM-13  $IC_{50}$  = 2.0 nM  
LLE = 8.06

**Binding Mode.** Crystal structures of “compound 19” bound with DHODH (**PDB:8DHG**) highlight some crucial interactions around the triazolone ring. The analog “compound 29” (**PDB:8DHH**), with a 4-amino pyridine rather than 3-amino pyridine in the scaffold, interacts with Leu67 and Tyr38 via a water network. These additional interactions might explain the slightly higher biochemical potency of “compound 29” (0.3 vs. 1.1 nM). Although potency was better for “compound 29”, its solubility (5  $\mu\text{M}$ ) ruled it out as a candidate.

**Preclinical Pharmacology.** Human AML xenograft mice were dosed with 10 and 20 mg/kg of “compound 19” QD for 5 days. Treatment resulted in a tumor growth inhibition of 44% (10 mg/kg) and 60% (20 mg/kg;  $P=0.0031$ ). The compound did not cause a significant impact on body weight over the 5 day period.

**Clinical Development.** Preclinical compound.

**Patent.** Janssen has filed a US patent application ([US20220089568A1](#)) that describes “compound 19” and other *N*-heterocyclic 3-pyridyl carboxamide inhibitors.

oral DHODH inhibitor

tumor growth inhibition in xenograft models

from virtual screening and SBDD

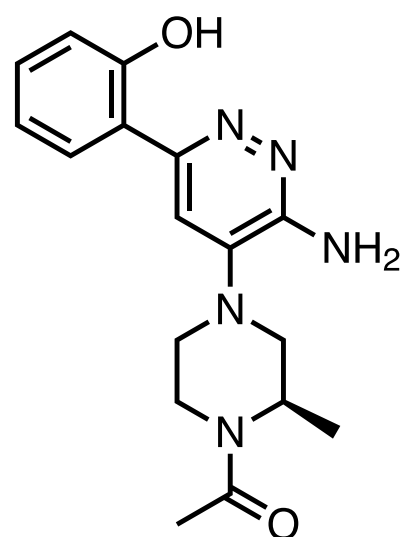
*J. Med. Chem.*

Janssen, Spring House, PA

featured article: <https://doi.org/10.1021/acs.jmedchem.2c00788>

# GNE-064

## SMARCA2/4 and PBRM1



**Context.** [GNE-064](#) (Genentech) is an oral inhibitor of the [bromodomains](#) of SMARCA2/4 and PBRM1 being developed as a tool compound. Many proteins contain bromodomains (there are 61 in the human genome), which recognize acetyl lysines and are involved in regulating gene transcription. Proteins that contain bromodomains are [often mutated in cancers](#), and bromodomains are considered to be important drug targets in a variety of cancers, with [several such compounds](#) targeting BET-family and CREBBP/EP300 bromodomains having made it into the clinic. Despite being the least druggable bromodomain proteins as [predicted by binding pocket structural analysis](#) and [challenges](#) with identifying strong enough probes, SMARCA2/4 tool compounds have been developed, such as [PFI-3](#) and GNE-064.

**Target.** Acetylation of lysine residues on histones and other chromatin-associated factors is an essential post-translational modification. [Bromodomains](#) are a class of protein domains that “read” or recognize acetyl-lysine residues on proteins. In addition to mediating histone acetylation, bromodomains also play a [role](#) in chromatin remodeling and recruitment of other factors necessary for transcription. In humans, the 61 bromodomains that have been [identified have been classified](#) into eight family members. [Small molecule analogues](#) of acetylated lysine have been found to preclude the binding of target substrates at the bromodomain binding pocket and disrupt cellular localization. GNE-064 is one of such tool ligands and targets three bromodomains VIII family involved in chromatin remodeling and repair: [SMARCA2 and SMARCA4](#), and a bromodomain of the [PBAF](#) signature subunit PBRM1.

**Mechanism of Action.** Some bromodomain inhibitors [bind](#) to the strongly hydrophobic pocket of the protein, leading to eviction of the bromodomains from chromatin. For bromodomains that do not directly interact with chromatin, binding of an inhibitor disrupts the interaction of the protein with acetylated histones. Due to the involvement of the [bromodomains](#) of SMARCA2, SMARCA4, and PBRM1 in chromatin remodeling, inhibition of their function is expected to be [lethal](#) for malignant cells.

**Hit-Finding Strategy.** [A library of ~43,000 compounds](#) was screened in a TR-FRET assay in which the small molecule competes for peptide binding within the SMARCA4 bromodomain. “Compound 1” showed modest activity ( $IC_{50} = 5.3 \mu M$ ), which was further validated by ITC and exhibited promising selectivity for SMARCA2 ( $4.3 \mu M$ )/4 and PBRM1 ( $3.1 \mu M$ ) over BRD4 ( $>100 \mu M$ ). A cocrystal structure of “compound 1” bound to the SMARCA4 bromodomain showed a bidentate H-bonding interaction between Asn1540, aniline moiety, and N2 of the aminopyridazine.

oral SMARCA2/4 and PBRM1 selective inhibitor

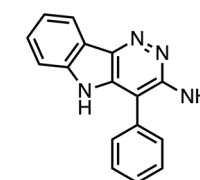
oral PK observed in mouse

from 43k cmps HTS and SBDD

*J. Med. Chem.*

Genentech, South San Francisco, CA

featured article: <https://doi.org/10.1021/acs.jmedchem.2c00662>



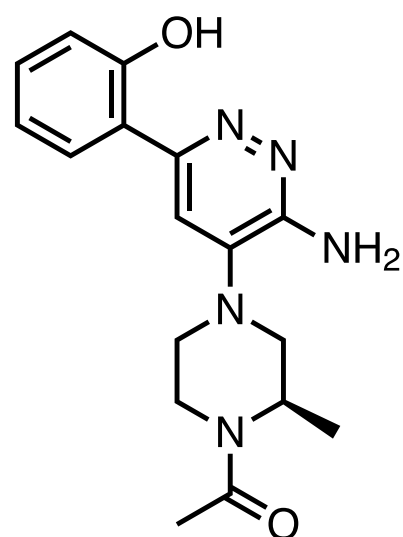
**Compound 1**

SMARCA4  $IC_{50} = 5.3 \mu M$

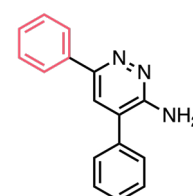
BRD4  $IC_{50} >100 \mu M$

# GNE-064

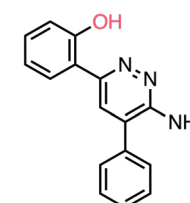
## SMARCA2/4 and PBRM1



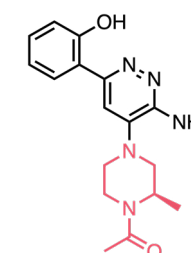
**Lead Optimization.** The series optimization started with “compound 2”, which substituted the indole in “compound 1” for a phenyl moiety. This provided a more synthetically amenable scaffold and allowed for more options to explore SAR. Introduction of a 2-hydroxyl group at the phenyl ring imparted a 177-fold improvement in potency in “compound 4” (0.03 μM) compared to “compound 1” (5.3 μM) and 1900-fold increase when compared to “compound 2” (57.1 μM). Through x-ray crystallography and modeling studies, it was found that the phenolic hydroxyl group in “compound 4” engages in a network of key hydrogen bonding interactions within the SMARCA4 binding pocket. Despite promising cellular potency and high selectivity for family VIII bromodomains, “compound 4” had limited solubility (11 μM) and poor metabolic stability (data not reported). In an effort to maintain potency while reducing lipophilicity, GNE-064 (“compound 5”) results from replacing the phenyl moiety attached at the 2-position of the pyridazine in “compound 4” with an acetylated piperazine. GNE-064 retained the high potency for SMARCA2/4 and PBRM1, exhibited greater than 250-fold selectivity vs BRD4, and improved solubility and pharmacokinetic properties (Hep Cl in rats <10 mL/min/kg).



**Compound 2**  
SMARCA4 IC<sub>50</sub> = 57.1 μM  
BRD4 IC<sub>50</sub> >100 μM



**Compound 4**  
SMARCA4 IC<sub>50</sub> = 0.03 μM  
BRD4 IC<sub>50</sub> = 27 μM  
kinetic solubility = 11 μM



**GNE-064**  
SMARCA4 IC<sub>50</sub> = 0.035 μM  
BRD4 IC<sub>50</sub> = 34 μM  
kinetic solubility = 120 μM

**Binding Mode.** The crystal structure (PDB:7TAB) released by the study authors shows some essential features of the binding mode of the analog “compound 4” and SMARCA4. The aminopyridazine moiety forms a bidentate hydrogen-bonding interaction with Asn1540. Another relevant characteristic is the role of the phenolic hydroxyl group and its hydrogen bond with Tyr1497 residue. The inhibitor engagement leads to the displacement of the water molecule in the binding site, and the non-replacement of water-Tyr1497 interaction leads to loss of affinity due to the structural water network disruption. This role can be exemplified in the SMARCA4 biochemical potency measured between “compound 2” (57100 nM) and “compound 4” (30 nM).

**Preclinical Pharmacology.** GNE-064 demonstrated sub-micromolar potency against the bromodomains of SMARCA2 (0.01 μM), SMARCA4 (0.010 μM) and PBRM1 bromodomain 5 (0.018 μM). In mouse PK studies, a low unbound plasma clearance of 16 mL/min/kg, C<sub>max</sub> = 1.0 μM, t<sub>1/2</sub> = 1.1 h, steady state V<sub>d</sub> = 1.0 L, and oral bioavailability of 59% was observed for GNE-064.

**Clinical Development.** Preclinical compound.

**Patent.** GNE-064 has been described in [US10308614B2](#), which was granted in June 2019 and is valid until February 2036.

oral SMARCA2/4 and PBRM1 selective inhibitor

oral PK observed in mouse

from 43k cmps HTS and SBDD

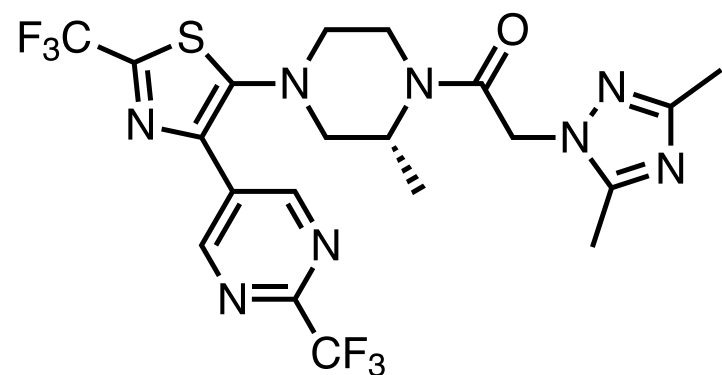
*J. Med. Chem.*

Genentech, South San Francisco, CA

featured article: <https://doi.org/10.1021/acs.jmedchem.2c00662>

# ACT-660602

## CXCR3



**Context.** [ACT-660602](#) (Idorsia Pharmaceuticals) is an oral chemokine receptor CXCR3 antagonist being developed for autoimmune diseases. Chemokines and their receptors make up the signaling system that is responsible for immune cell migration. This is important for the innate immune system's ability for fighting infection, but dysregulation of these pathways can lead to autoimmune disorders, especially when T cells migrate into inflamed tissue and cause tissue and organ damage. Since the identification of CXCR3 in [1996](#) and findings that its [overexpression led to cell migration](#), CXCR3 has been implicated in a [number of diseases](#), driving the search for potent antagonists. However, only three drugs have been approved for chemokine receptors so far: [CXCR4 antagonist plerixafor](#), [CCR5 antagonist maraviroc](#), and anti-CCR4 mAb [mogamulizumab](#). The non-competitive CXCR3 compound SCH546738 showed promising [preclinical efficacy in rodent models](#), similar to another CXCR3 antagonist [NBI74330](#), but were not brought to clinical trials. CXCR3 antagonist [AMG487](#) reached Ph. IIa for psoriasis patients but failed to reach its endpoints and no further clinical development has been reported since in other indications. Currently, along with ACT-660602, Idorsia is also developing another CXCR3 antagonist [ACT-672125](#) for autoimmune diseases.

**Target.** [CXCR3](#), a chemokine receptor and a GPCR, is expressed on various immune cells and expressed under inflammatory conditions by the chemokine ligands CXCL9, CXCL10, and CXCL11. Involvement of the protein in autoimmune diseases, through creation of local amplification loops of inflammation in target organs, is [well-documented](#). For instance, overexpression of the protein has been implicated in [rheumatoid arthritis](#), [multiple sclerosis](#), [transplant rejection](#), and [atherosclerosis](#).

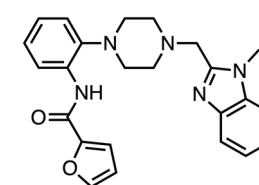
**Mechanism of Action.** Antagonism of CXCR3 function [leads](#) to inhibition of immune cell migration and reduction of inflammation. Previous CXCR3 antagonists have been [associated with](#) effects such as reduced inflammation and cartilage damage, attenuated atherosclerotic plaque formation, prolonged allograft survival, and reduced lung metastasis.

**Hit-Finding Strategy.** A high-throughput screen of the Actelion-Idorsia library led to the discovery of "compound 1" ( $IC_{50} = 372$  nM), which had sub-micromolar activity against FLIPR in a calcium mobilization assay using CXCL10 as the agonist.

oral CXCR3 antagonist  
efficacy in mice model of lung inflammation  
from HTS and opt  
*J. Med. Chem.*

Idorsia Pharmaceuticals Ltd., Allschwil, CH

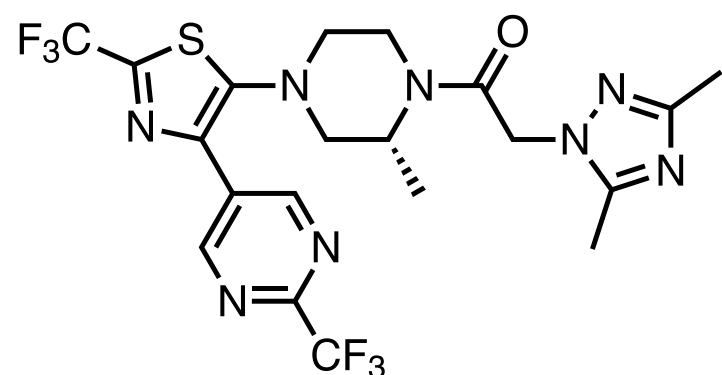
featured article: <https://doi.org/10.1021/acs.jmedchem.2c00675>



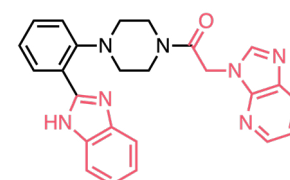
**Compound 1**  
FLIPR  $IC_{50} = 372$  nM

# ACT-660602

## CXCR3

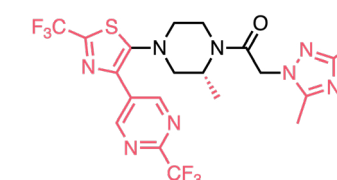


**Lead Optimization.** During the hit-to-lead phase, “compound 1” was modified by installing a 4-azabenzimidazole substituent via an acetyl linker and exchanging the furan amide from with a benzimidazole to yield a promising compound (“compound 3”) with high aqueous solubility and improved biological activity (~ 87-fold). However, “compound 3” suffered from high potency hERG inhibition. Through a series of lead optimizations, a thiazole was selected as the core heterocycle with two trifluoromethyl substituents to improve metabolic stability and high potency in three bioassays. Lastly, a dimethyltriazole was installed for reduced clearance and improved oral exposure culminating in ACT-660602.



**Compound 3**

FLIPR IC<sub>50</sub> = 4.3 nM  
hERG IC<sub>50</sub> = 0.66 μM



**ACT-660602**

FLIPR IC<sub>50</sub> = 2.7 nM  
hERG IC<sub>50</sub> >20 μM

**Binding Mode.** Structure not disclosed.

**Preclinical Pharmacology.** A mouse model of acute lung inflammation induced by nebulized lipopolysaccharide was used to evaluate the effect of ACT-660602 on CXCR3–CXCR3 ligand interaction-mediated migration of leukocytes to the lungs. Mice treated with ACT-660602 orally for 3 days (30 mg/kg QD) showed a 39% reduction in CXCR3<sup>+</sup> T cells and a 65% reduction in CXCR3<sup>+</sup> CD8<sup>+</sup> T cells compared to the vehicle group. Target engagement studies showed a mean target engagement at steady-state of 68%. Despite these positive data, the compound was also found by Idorsia Pharmaceuticals scientists to be an exclusive CYP2D6 substrate. CYP2D6 is [highly polymorphic](#) in humans, often causing drugs metabolized through this pathway to have [widely variable plasma concentrations](#).

**Clinical Development.** Preclinical compound.

**Patent.** ACT-660602 and a series of 1-(piperazin-1-yl)-2-([1,2,4]triazol-1-yl)-ethanone derivatives were described by Idorsia Pharmaceuticals Ltd in the patent [WO2015011099A1](#). The US patent [US10259807B2](#) was granted in April 2019, and is valid until July 2034.

oral CXCR3 antagonist

efficacy in mice model of lung inflammation

from HTS and opt

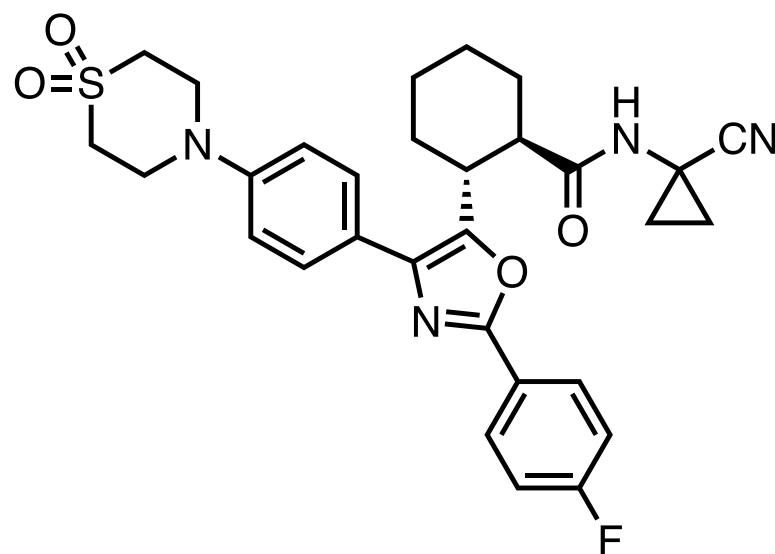
*J. Med. Chem.*

Idorsia Pharmaceuticals Ltd., Allschwil, CH

featured article: <https://doi.org/10.1021/acs.jmedchem.2c00675>

# Compound 23

## Cat K



**Context.** “Compound 23” (Merck) is a selective oral cathepsin K (CatK) inhibitor intended for osteoarthritis. **Osteoarthritis** affects around 15% of the population, and current treatments offer only symptom relief, highlighting the need for targeted treatments. Prior to the “compound 23”, several CatK inhibitors had reached **clinical development**: **relacatib** (GSK), **balicatib** (Novartis), **ONO-5334** (Ono Pharmaceuticals), and **odanacatib** (Merck). Merck’s preclinical compound **MK-1256** was only 40-fold selective, so they set out to develop a compound with at least 1000-fold selectivity for CatK over other **biologically relevant cathepsins**, using MK-1256 as a starting point.

**Target.** **CatK is a dimeric** collagen-degrading cysteine protease and plays a key role in bone resorption by osteoclasts. Upregulation of the enzyme has been **observed** in articular cartilage of transgenic, implying a role in osteoarthritis, while its inhibition in animal models was **associated with** reduced cartilage degeneration. **CatK’s importance** as a drug target was noted based on observations of patients with a loss-of-function CTSK gene (**pseudoyostosis**, an autosomal recessive inheritance) showing signs of osteosclerosis, reduced bone turnover and undigested mineral matrices, phenotypes that were mimicked in CTSK knockout mouse models. These observations in pseudoyostosis patients led to various animal studies demonstrating the utility of CatK inhibitors in attenuating arthritic diseases. For example, administration of the **CatK inhibitor relacatib** to ovariectomized female monkeys, who are models of postmenopausal osteoporosis, was shown to decrease bone resorption and serum levels of collagen peptides. Key challenges in targeting CatK for osteoarthritis treatment include selectivity over other cathepsins. **CatK preferably cleaves** helical domains of type I collagen, which makes up 90% of organic bone matrix. In fact, CatK is able to cleave 100% of type I bone collagen compared to 57%, 36%, and 37% cleavage of other cathepsins CatS, CatL, and CatB.

**Mechanism of Action.** The exact role of CatK and the underlying mechanisms in bone and other diseases have not **been fully elucidated**. However, CatK inhibitors targeting osteo/chondroclasts, chondrocytes, or synoviocytes are expected to cripple the enzyme’s **involvement** in processes such as bone resorption, subchondral bone, and cartilage remodeling.

**Hit-Finding Strategy.** A reversible CatK inhibitor, **MK-1256** ( $IC_{50} = 1.8$  nM), was previously identified through rational optimization of an **initial hit**, using a functional bone resorption assay. Although MK-1256 exhibited high potency and selectivity against most biologically relevant cathepsins, it was selected as a starting point for development to improve selectivity against CatF.

oral CAT K inhibitor

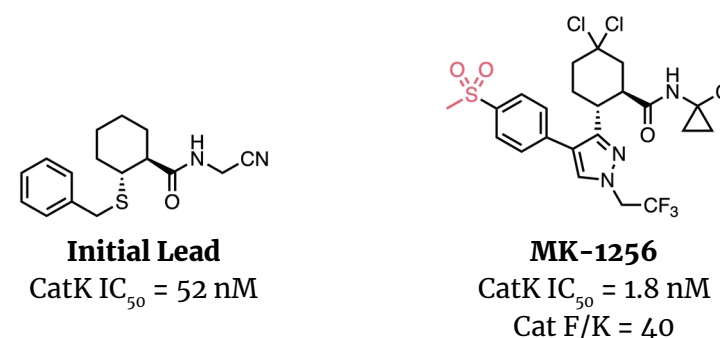
reduced uCTX-I levels in dog model

from opt of a previously disclosed cmpd

*Bioorg. Med. Chem. Lett.*

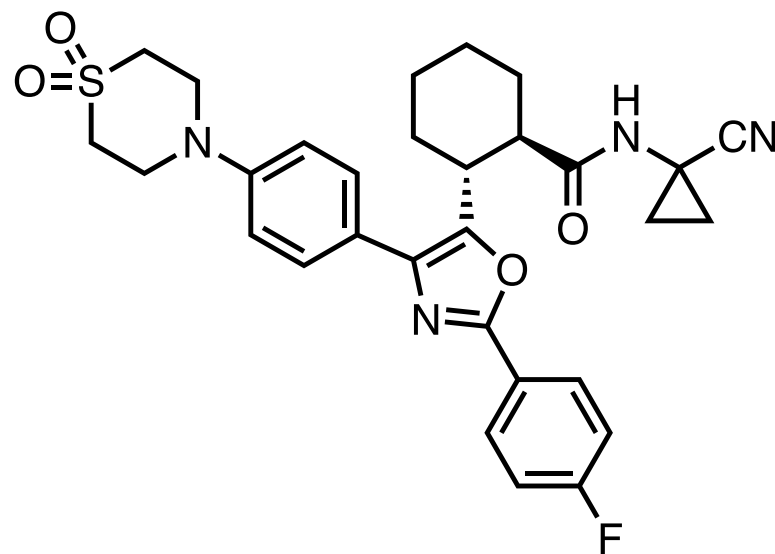
Merck, West Point, PA

featured article: <https://doi.org/10.1016/j.bmcl.2022.128927>

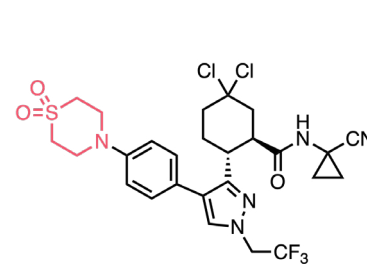


# Compound 23

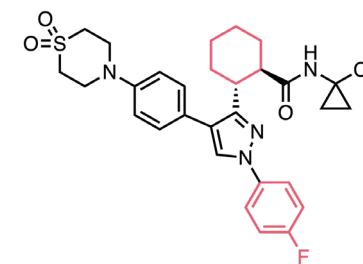
## Cat K



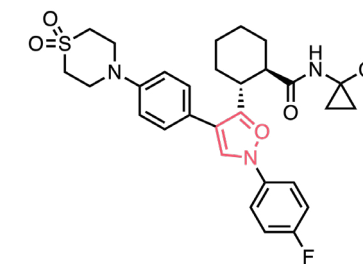
**Lead Optimization.** Optimization focused on maintaining potency ( $IC_{50}$  values) as measured by a human CatK inhibition assay and selectivity (CatF/K ratio) via a humanized rabbit CatK inhibition assay. Modifying the methyl sulfone to the thiomorpholine dioxide in “compound 4” exhibited not only an 8-fold increase in selectivity but also a 4-fold increase in CatK activity when compared to MK-1256. This bulkier substitution is hypothesized to more fully occupy the S3 binding pocket of CatK, leading to enhanced selectivity and potency. Other key changes included the removal of a geminal dichloro substitution on the cyclohexyl ring and the addition of an N-arylation on the pyrazole leading to subnanomolar potency with >1000-fold selectivity in “compound 10”. However, the dihydrocyclohexyl moiety in “compound 10” was more prone to oxidative metabolism and thus required the replacement of the pyrazole with an oxazole ring to improve intrinsic clearance in rat liver microsomes.



**Compound 4**  
CatK  $IC_{50}$  = 0.5 nM  
Cat F/K = 314



**Compound 10**  
CatK  $IC_{50}$  = 0.5 nM  
Cat F/K = 1000  
 $Cl_{int}$  = 41 ml/min/kg



**Compound 23**  
CatK  $IC_{50}$  = 0.5 nM  
Cat F/K = 1460  
 $Cl_{int}$  < 30 ml/min/kg

**Binding Mode.** Structure not disclosed.

**Preclinical Pharmacology.** “Compound 23” had a dose-dependent inhibitory effect on urinary C-telopeptide of collagen type I (uCTX-I) levels in a canine model of osteoporosis. The efficacious dose for Cat K inhibitors is generally determined by full reduction of uCTX-I, a [validated biomarker](#) for osteoporosis in animal models. Here, a dose of 0.3 or 15 mg/kg of “compound 23” daily for four days produced an 81% and 91% reduction, respectively.

**Clinical Development.** Preclinical compound.

**Patent.** “Compound 23” and other cathepsin cysteine protease inhibitors were described in patent [WO2015120580A1](#) assigned to Merck Sharp and Dohme Corp. The US patent [US9656990B2](#) was granted in May 2017 and is valid until February 2035.

oral CAT K inhibitor

reduced uCTX-I levels in dog model

from opt of a previously disclosed compd

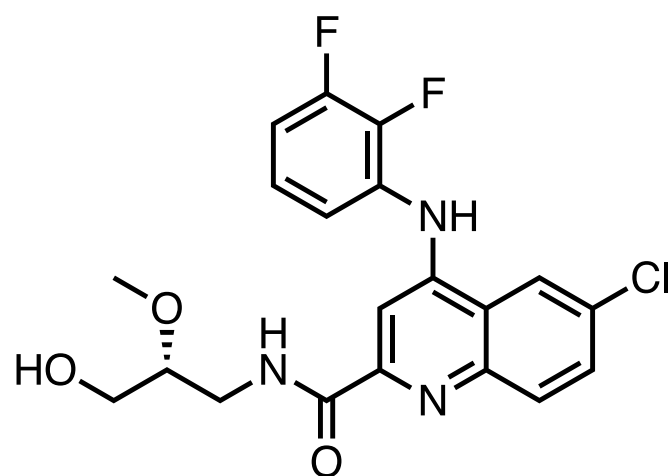
*Bioorg. Med. Chem. Lett.*

Merck, West Point, PA

featured article: <https://doi.org/10.1016/j.bmcl.2022.128927>

# Compound 7

## 20S proteasome



**Context.** “Compound 7” (NIBR) is an oral *Trypanosoma brucei* 20S proteasome inhibitor being developed for Human African Trypanosomiasis (HAT). **African sleeping sickness**, or HAT, is caused by a parasite in the genus **Trypanosoma**. The parasite is spread by the Tsetse fly, and the lifecycle of the parasite involves a phase in the blood of the host, followed by a devastating phase in the brain of the host. Melarsoprol, the prodrug of **arsenic-containing melarsen oxide**, was the **first treatment** for second-phase HAT since 1942 but was highly neurotoxic and **brought widespread resistance** in the 1990s. In 2009, the **introduction of NECT**, nifurtimox, an antiparasitic for Chagas disease caused by *T. cruzi*, combined with IV administration of eflornithine, an irreversible inhibitor of ornithine decarboxylase, then became the standard-of-care but the WHO later recommended in 2019 that the oral nitroimidazole **fexinidazole** be used. However, cross-drug resistance remains a concern as the **resistance potential** of nifurtimox-treated *T. brucei* to fexinidazole is ~27-fold. The ability of new drugs to cross the blood-brain barrier poses an additional challenge.

**Target.** The parasitic proteasome was **validated as a target** during a screen of 3 million compounds on the proliferation of *Leishmania donovani*, *T. cruzi*, and *T. brucei*. By evolving drug-resistant parasite strains over 12 months, a homozygous mutation in the proteasome gene encoding the  $\beta$ -4 subunit was identified. Additional validation came from the **structural-based design** of protease inhibitors as antiparasitics to treat the malarial parasite *Plasmodium falciparum*. The 20S proteasome is essential for the rapid turnover of non-functional, oxidized, and misfolded proteins. In addition, *T. brucei* shows **structural** and **functional** differences from the human proteasomes allowing for a larger therapeutic window.

**Mechanism of Action.** “Compound 7”, a *T. brucei* 20S proteasome inhibitor, binds to the region between two of the enzyme’s subunits, one of which is a catalytic subunit. Ultimately, the enzyme’s ability to catalyze ubiquitination of parasitic proteins and ensure their degradation is blocked.

**Hit-Finding Strategy.** “Compound 1” was identified as a singleton hit from biochemical HTS screen of 3 million compounds against the 20S proteasome of *Leishmania tarentolae*, a protozoan parasite **that lends itself** to biochemical manipulation. It showed promising chymotrypsin inhibition in *T. b. brucei*, a **subspecies of the parasite that is often used in experimental models of HAT**, but is non-human pathogenic. Furthermore, “compound 1” presented an attractive in vitro ADME profile (high passive permeability and low P-gp efflux), which was seen as an ideal starting point for optimization, especially for a compound that would require brain penetration.

oral 20S proteasome inhibitor

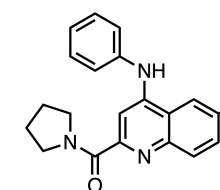
efficacy in stage II mouse model of HAT

3 million cmpd HTS and SBDD

*J. Med. Chem.*

Novartis Institutes for Biomedical Research,  
Emeryville, CA

featured article: <https://doi.org/10.1021/acs.jmedchem.2c00791>



**Compound 1**

*T. b. brucei* EC<sub>50</sub> = 360 nM

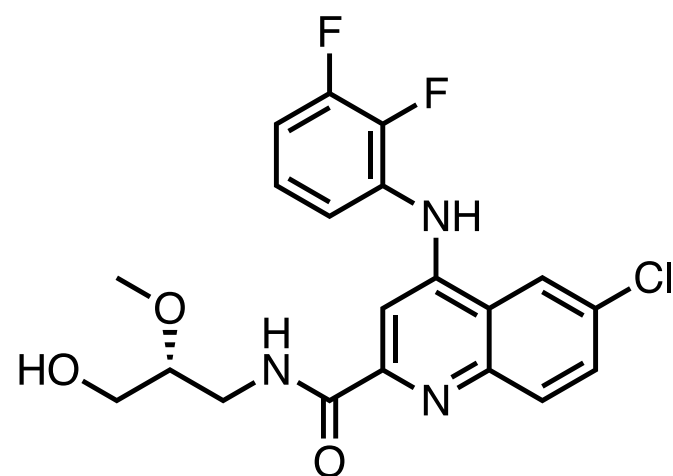
*T. b. b/hu* 20S proteasome IC<sub>50</sub> = 764/>10000 nM

LM CL<sub>int</sub> M/R/H = 330/76/11  $\mu$ L/min/mg

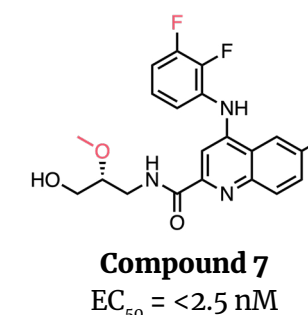
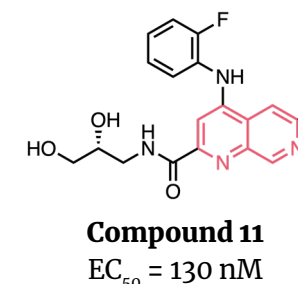
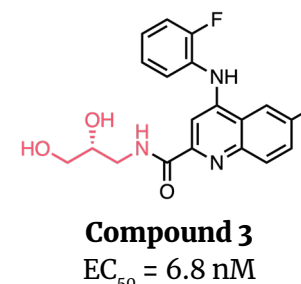
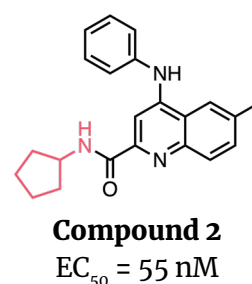
MDCK-MDR1 A to B (ER) = 18.4 (0.6)

# Compound 7

## 20S proteasome



**Lead Optimization.** A series of different secondary and tertiary amines were screened as a substitute for the pyrrolidine, with the former showing the most promise (“compound 2”). This improvement was rationalized through the use of computational modeling and a cryo-EM structure of “compound 2” bound with the 20S proteasome of *L. tarentolae*. Initial exploration of aliphatic carbocycles gave molecules with low metabolic stability, so polarity was increased on the sidechain, leading to the use of an aminopropanediol (“compound 3”). Further optimization, guided by the cryo-EM structure, demonstrated the importance of electron-poor anilines, especially those with an *ortho*-fluorine. Insertion of an additional nitrogen to the quinoline core improved solubility and liver microsome clearance but unfortunately led to a decrease in activity and permeability (“compound 11”). In order to better predict which compounds would have an optimal brain-to-plasma coefficient ( $K_p$ ), an in silico model, provided through [StarDrop](#), was developed. The most promising compounds were selected for mouse brain PK, plasma protein binding, and brain tissue binding studies. Ultimately, “compound 7” proved to have the best in vivo profile, and was able to cure a stage II mouse model of HAT.



**Binding Mode.** The cryo-EM structure of an analog, “compound 2”, bound to the *L. tarentolae* 20S proteasome pocket (PDB:7ZYJ), revealed three main interactions. An intramolecular H-bond between the amide N–H and quinoline nitrogen restricts the conformation of the “tail”, allowing it to fit within the channel pocket of the binding site; a  $\pi$ -stacking interaction of the quinoline aromatic system with Phe24; and an aniline hydrogen bond with the phenol in Tyr113.

**Preclinical Pharmacology.** “Compound 7” completely cleared the blood parasites induced in mouse models of stage I HAT (hemolymphatic mouse model) and stage II HAT (meningo-encephalic mouse model), with an efficacious dose of 3 mg/kg QD and 15 mg/kg BID for each model, respectively. hERG binding and automated patch clamp (q-patch) signals were monitored to assess potential proarrhythmic potential, with “compound 7” showing the best safety profile, attributed to the 6-substituent on the quinoline. With a safety margin for hERG judged to be sufficient based on EC<sub>50</sub>/free mouse C<sub>max</sub>, the molecule was selected for broader toxicology assessment. A subsequent 7-day oral gavage study, in rats, showed that only the bone marrow had potential toxicity effects, and only at the highest tested dose (300 mg/kg/day).

**Clinical Development.** Preclinical compound.

**Patent.** No publicly available records as of 20 September 2022.

oral 20S proteasome inhibitor  
efficacy in stage II mouse model of HAT

3 million compd HTS and SBDD

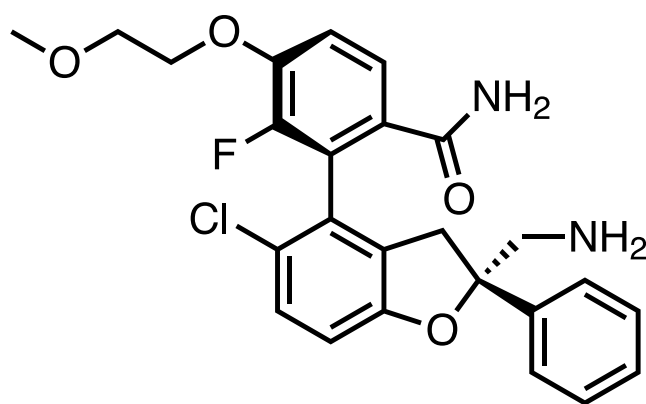
*J. Med. Chem.*

Novartis Institutes for Biomedical Research,  
Emeryville, CA

featured article: <https://doi.org/10.1021/acs.jmedchem.2c00791>

# Compound 6

## YAP-TEAD

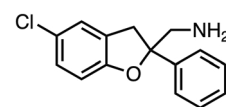


**Context.** “Compound 6” (Novartis) is a first-in-class YAP-TEAD protein-protein inhibitor. The TEAD transcription factor and its coactivator YAP and WWTR1/TAZ of the [Hippo pathway](#) are responsible for directly regulating the expression of genes involved in cell proliferation and organ size. Several kinases in the cascade have recently gained attention as [potential therapeutic targets](#) for certain cancers. The interaction between YAP and TEAD is important for Hippo signaling, which is [dysregulated in some cancers](#), and disrupting this interaction could be a therapeutic strategy for suppressing Hippo-mediated proliferation. To date, the only published small molecules that attempt to directly target the YAP-TEAD protein-protein interface have shown weak activity, although several have been [reported](#) that inhibit TEAD auto-palmitoylation, including one of [April 2021’s MOTM](#), [VT-104](#). In this study, a hit discovered in a virtual screen showed weak activity, and optimization led to the title compound with nearly 1000-fold greater activity than the original hit.

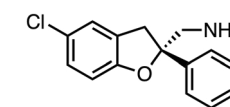
**Target.** The Hippo signaling pathway regulates physiological processes such as homeostasis and tissue regeneration. As dysfunction in this pathway has been observed in various cancers and [other diseases](#), disruption of the protein-protein interaction of YAP and TEAD in the Hippo pathway blocks TEAD signaling and is considered to be a [potential therapeutic event](#). The disruption of YAP and TEAD has been known to be a drug discovery challenge due to an overall extended protein-protein interface of 25 Å and the shallow depth of two protein-protein interaction interface pockets. Therefore, a few micromolar YAP-TEAD protein-protein [small molecules inhibitors](#) have been disclosed in the literature. Some of these compounds have been able to impair the TEAD-dependent transcriptional activity in vitro assays resulting [in the arrest of cell migration and proliferation](#).

**Mechanism of Action.** YAP interacts mainly through two shallow and large molecular binding sites, the TEAD  $\alpha$ -helix and  $\Omega$ -loop pockets. In a previous study with small peptides, the authors showed that targeting just one of these sites, near Glu391 residue ([PDB:6Q36](#)), in the deep  $\Omega$ -loop pocket, with a 6-chlorotryptophan warhead could lead to the complete YAP-TEAD disruption and subsequently precluding the expression of pro-proliferative genes activated by the Hippo pathway.

**Hit-Finding Strategy.** Previous work from Novartis scientists [focused](#) on peptidic inhibitors of the YAP-TEAD interaction, ultimately [finding](#) a 15-mer peptide with nanomolar biochemical potency that mimicked the  $\Omega$ -loop sequence of YAP. Key to the activity was the presence of 6-chlorotryptophan, which was shown to occupy the deepest part of the  $\Omega$ -loop pocket ([PDB:6Q36](#)). Using 6-chloroindole or a chlorophenyl moiety as a core constraint option, a [GLIDE docking study](#) was performed using the Novartis collection, leading to a selection of ~500 compounds. These compounds were biochemically assessed in a TR-FRET assay which measured their ability to inhibit the YAP-TEAD interaction. The most active compound identified was “compound 1”, a racemate, which produced a 50% inhibition at a concentration of 500  $\mu$ M. The active enantiomer, “compound 2”, had an  $IC_{50}$  value of 267  $\mu$ M.



Compound 1



Compound 2  
 $IC_{50} = 267 \mu$ M

YAP-TEAD PPI inhibitor

single digit nanomolar potency

virtual screening and SBDD

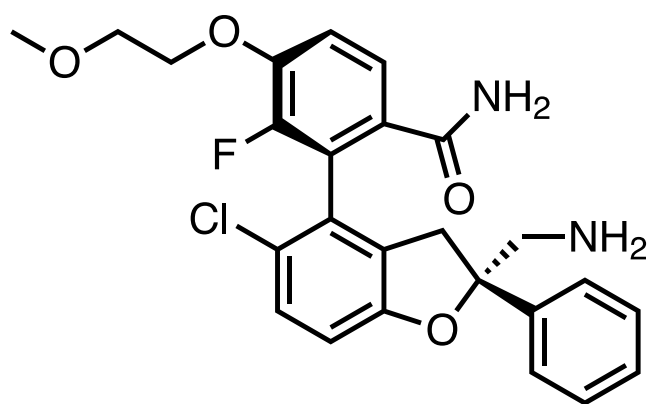
ChemMedChem

Novartis, Basel, Switzerland

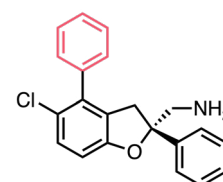
featured article: <https://doi.org/10.1002/cmdc.202200303>

# Compound 6

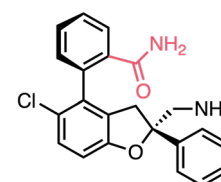
## YAP-TEAD



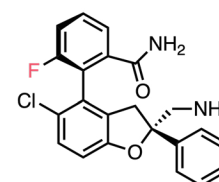
**Lead Optimization.** A crystal structure of “compound 2” bound to TEAD (**PDB:8A0V**) indicated that expansion into the  $\Omega$ -loop pocket, by substitution at position 4 of the dihydrobenzofuran, would allow for favorable hydrophobic interactions with the sidechains of I271, L296, and V266. A phenyl substituent at this position was considered particularly attractive since it could potentially form van der Waals interactions with these residues. The potency of “compound 3” is two orders of magnitude higher ( $IC_{50} = 3.1 \mu M$ ) than “compound 2”, validating this hypothesis. Further analysis of the crystal structure suggested that modification of the two *ortho* positions and one of the *meta* positions on the benzene may drive potency. This was indeed the case, as the addition of an *ortho* amide (“compound 4”) and fluoride (“compound 5”) moiety and a *meta* 2-methoxyethoxy substituent (“compound 6”) sequentially improved potency.



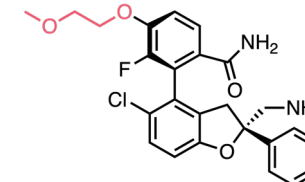
**Compound 3**  
 $IC_{50} = 3.1 \mu M$



**Compound 4**  
 $IC_{50} = 0.15 \mu M$



**Compound 5**  
 $IC_{50} = 0.027 \mu M$



**Compound 6**  
 $IC_{50} = 0.0027 \mu M$

**Binding Mode.** The X-ray crystal structure (**PDB:8A0U**) of “compound 4” bound with TEAD3 shows that interaction occurs in the  $\Omega$ -loop pocket. Hydrophobic contacts can be observed between the dihydrobenzofuran core and Val415. Other relevant interactions include a salt bridge interaction between the aminomethyl group and Glu417, a face-to-edge aromatic interaction with the 2-phenyl substituent and Trp300, and hydrogen bonds between the amide group with Gln270 and Lys274.

**Preclinical Pharmacology.** In vitro cellular assays evaluating the inhibition of YAP/TEAD-dependent reporter gene expression in NCI-H2052 cells showed an  $IC_{50}$  of 51 nM. In YAP-deleted MKN-45 cells, the compound demonstrated no inhibitory effects up to 10  $\mu M$ . Additional preclinical data, including in vivo efficacy data, are yet to be reported by Novartis scientists.

**Clinical Development.** Preclinical compound.

**Patent.** Novartis' newly disclosed YAP-TEAD PPI biaryl inhibitors series has been described in the patent [WO2021186324A1](#). The US patent ([US20210299100A1](#)) has been filed by Novartis and is currently pending.

YAP-TEAD PPI inhibitor

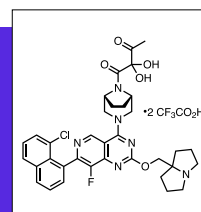
single digit nanomolar potency

virtual screening and SBDD

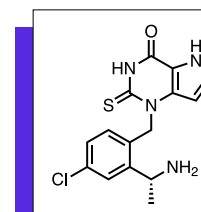
ChemMedChem

Novartis, Basel, Switzerland

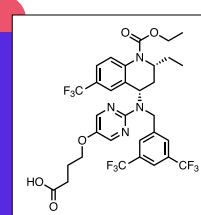
featured article: <https://doi.org/10.1002/cmdc.202200303>

**Compound 3 | KRAS<sup>G12R</sup>**

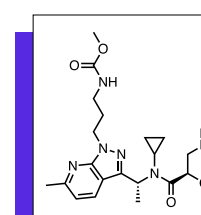
KRAS<sup>G12R</sup> mutant-selective covalent inhibitor  
privileged arginine-reactive functional group  
from previously disclosed KRAS inhibitors  
*J. Am. Chem. Soc.*  
UCSF, San Francisco, CA

**AZD4831 | MPO**

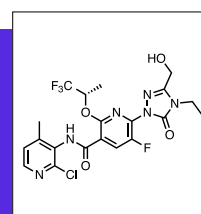
oral MPO covalent inhibitor  
Ph. IIb/III candidate in HFpEF  
previous literature and selectivity opt  
*J. Med. Chem.*  
AstraZeneca, Gothenburg, SE

**Obicetrapib | CETP**

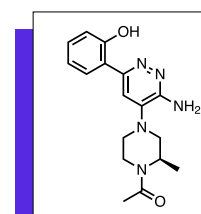
oral CETP inhibitor  
Ph. III candidate in cardiology  
Signif. lipid lowering effect at 5 mg PO QD  
*Nat. Med.*  
Monash University, Clayton, AU  
NewAmsterdam Pharma B.V., Naarden, NL

**SPH3127 | Renin**

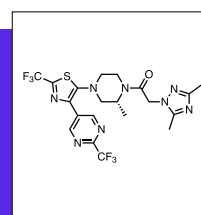
oral Renin Inhibitor  
Ph. III candidate in essential hypertension  
SBDD and PK profile opt  
*J. Med. Chem.*  
Mitsubishi Tanabe, Yokohama, JP  
Shanghai Pharmaceuticals, Shanghai, CN

**Compound 19 | DHODH**

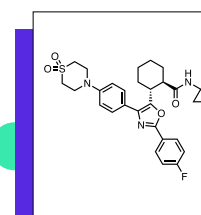
oral DHODH inhibitor  
tumor growth inhibition in xenograft models  
from virtual screening and SBDD  
*J. Med. Chem.*  
Janssen, Spring House, PA

**GNE-064 | SMARCA2/4 and PBRM1**

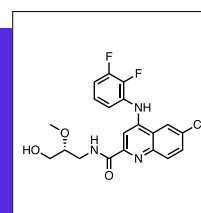
oral SMARCA2/4 and PBRM1 selective inhibitor  
oral PK observed in mouse  
from 43k cmps HTS and SBDD  
*J. Med. Chem.*  
Genentech, South San Francisco, CA

**ACT-660602 | CXCR3**

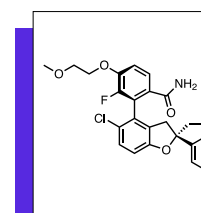
oral CXCR3 antagonist  
efficacy in mice model of lung inflammation  
from HTS and opt  
*J. Med. Chem.*  
Idorsia Pharmaceuticals Ltd., Allschwil, CH

**Compound 23 | Cat K**

oral CAT K inhibitor  
reduced uCTX-I levels in dog model  
from opt of a previously disclosed cmpd  
*Bioorg. Med. Chem. Lett.*  
Merck, West Point, PA

**Compound 7 | 20S proteasome**

oral 20S proteasome inhibitor  
efficacy in stage II mouse model of HAT  
3 million cmpd HTS and SBDD  
*J. Med. Chem.*  
Novartis Institutes for Biomedical Research,  
Emeryville, CA

**Compound 6 | YAP- TEAD**

YAP-TEAD PPI inhibitor  
single digit nanomolar potency  
virtual screening and SBDD  
*ChemMedChem*  
Novartis, Basel, Switzerland

**discover together**

[drughunter.com](https://drughunter.com)  
[info@drughunter.com](mailto:info@drughunter.com)